Heliyon 10 (2024) e31143

Contents lists available at ScienceDirect

Heliyon

journal homepage: www.cell.com/heliyon

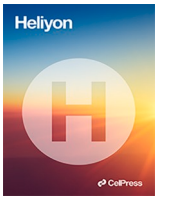

Research article

Effect of different drying methods on the structure and properties of porous starch

Yuanyuan Zhao [a,b,1], Simo Qiao [c,1], Xiaohui Zhu [b], Jinnan Guo [b], Guanqun Peng [b], Xiaoxia Zhu [b], Ruolan Gu [b], Zhiyun Meng [b], Zhuona Wu [b], Hui Gan [b], Dou Guifang [b,*], Yiguang Jin [a,b,**], Shuchen Liu [a,b,***], Yunbo Sun [a,b,****]

[a] Anhui Medical University, Hefei, 230000, China
[b] Beijing Institute of Radiation Medicine, Beijing, 100850, China
[c] Beijing Institute of Pharmacology and Toxicology, Beijing, 100850, China

ARTICLE INFO

Keywords:
Porous starch
Drying method
Supercritical carbon dioxide drying

ABSTRACT

In order to investigate the effects of different drying methods on the properties of porous starch. The present study used four drying methods, namely hot air drying (HD), spray drying (SPD), vacuum freeze drying (FD) and supercritical carbon dioxide drying (SCD) to prepare maize and kudzu porous starch. Findings indicated that the physicochemical properties (e.g., morphology, crystallinity, enthalpy value, porosity, surface area and water absorption capacity as well as dye absorption capacity, particle size) of porous starch were significantly affected by the drying method. Compared with other samples, SCD-treated porous starch exhibited the highest surface areas of the starch (2.943 and 3.139 m^2/g corresponding to kudzu and maize, respectively), amylose content (22.02 % and 16.85 % corresponding to kudzu and maize, respectively), MB and NR absorption capacity (90.63 %, 100.26 % and 90.63 %, 100.26 %, corresponding to kudzu ad maize, respectively), and thermal stability, whereas HD-treated porous starch showed the highest water-absorption capacity (123.8 % and 131.31 % corresponding to kudzu and maize, respectively). The dye absorption of the maize and kudzu porous starch was positively correlated with surface area, according to Pearson's correlation analysis. Therefore, in this study, our aim was to explore the effects of different drying methods on the Structure and properties of porous starch, and provide reference for selecting the best drying method for its application in different fields.

1. Introduction

Porous starch has been widely employed in pharmaceutical, chemical, and—in particular—food industries recently owing to its abundant pores and large specific surface area and pore volume [1]. Belingheri et al. [2] employed porous starch as a novel flavour carrier, plated tomato flavour onto the porous starch and spray dried it to achieve optimal performance of the flavour. Due to its

* Corresponding authors.
** Corresponding author. Beijing Institute of Radiation Medicine, Beijing, 100850, China.
*** Corresponding authors. Beijing Institute of Radiation Medicine, Beijing, 100850, China.
**** Corresponding author. Beijing Institute of Radiation Medicine, Beijing, 100850, China.
E-mail addresses: dougf@bmi.ac.cn (D. Guifang), jinyg@sina.com (Y. Jin), liusc118@163.com (S. Liu), sunyunbo0919@126.com (Y. Sun).
[1] These authors contributed equally to this research.

https://doi.org/10.1016/j.heliyon.2024.e31143
Received 14 January 2024; Received in revised form 8 May 2024; Accepted 10 May 2024
Available online 11 May 2024

excellent absorption performance, porous starch has recently also been widely used as an adsorbent for pollutants [3,4].

Thus far, several approaches, including physical, chemical, enzymatic, and synergistic methods, have been employed for synthesizing porous starch [5]. The enzymatic method is most commonly used owing to its mild reaction conditions, high catalytic efficiency, ecofriendliness, and specific substrate usage [6].

Porous starch is generally used in its dry form, which facilitates its processing, transportation, and storage. Therefore, appropriate drying equipment and process parameter settings play an important role in improving the quality and performance of the resulting products. Typical drying methods include hot-air drying (HD), vacuum freeze drying (FD), spray drying (SPD), supercritical carbon dioxide drying (SCD), and microwave drying [7].

HD, a widely utilized traditional drying method, is well-known for its simple process, short operation time, and stable product quality. However, owing to different applied temperatures, this method causes changes in the properties and structure of starch and deteriorates product quality [8].

To avoid the collapse of pores, FD employs the principle of the sublimation of frozen water, which involves gentle sublimation that does not require heating and enables the pores to maintain their original properties under vacuum conditions. However, long operation time, high energy consumption, and high investment costs have limited the usage of FD [9]. As previously reported [10], SPD is the most cost-effective method for industrial purposes as it allows extremely rapid solvent evaporation, leading to the rapid transformation of solutions or suspensions into solid products. This drying method avoids the collapse of pores in addition to preserving the porous texture of the processed material. Unfortunately, this method exhibits a lower yield than the other methods, such as FD.

Among the above-mentioned drying methods, SCD avoids the vapor–liquid interface and relatively low critical point of carbon dioxide, allowing better preservation of the original material structure. Therefore, SCD has been used to prepare porous materials with excellent properties, such as large surface areas, ultralow densities, and high porosities, with minimal damage to the microstructure [11]. Several studies have demonstrated the effects of different drying methods on the functional properties and chemical reactivity of starch and other materials [12–14]. For example, Zhang [15] reported that after the FD treatment, the surface morphology of potato starch granules changed and the orders of short- and long-chain molecules of the branched starch molecules reduced, resulting in a higher enzyme sensitivity of the product than that obtained in the case of HD treatment. Moreover, Zou [16] reported that starch prepared from maize, potato, and pea flours subjected to FD and SCD exhibited different structural and functional properties; SCD-treated starch gels exhibited higher density and much higher specific surface areas than those of cryogels.

However, attention has been scarcely paid to understand the effect of drying methods on the properties of porous starch. Hence, this study used α-amylase (AM) and glucoamylase (GAM) for preparing maize and kudzu porous starch from two different crystal types of starch (A-, C-type, respectively) and analyzed their properties after drying the hydrolysed starch using four drying methods. This study establishes a theoretical basis for optimizing the processing of porous starch through various drying methods.

2. Materials and methods

2.1. Materials

Maize starch was obtained from Shanghai Aladdin Biochemical Technology Co., Ltd. (Shanghai, China) and kudzu starch was kindly donated by Suzhou February Wind Foodstuffs Co.

Glucoamylase (GAM (100000 U/mL) and α-amylase (AM (≥500 KNU/g) were purchased from Shanghai Aladdin Biochemical Technology Co., Ltd. (Shanghai, China). Dibasic sodium phosphate, sodium hydroxide, and all other analytical-grade chemicals were purchased from Sinopharm Chemical Reagent Co. Ltd. (Suzhou, China).

2.2. Preparation of porous starch

Porous starch was prepared according to the method proposed by Davoudi et al. [17], with slight modifications. Notably, 10 g of maize and kudzu starch, with an initial moisture content of ~13 % and 17 %, respectively, were added to 250 mL of a citric acid–disodium hydrogen phosphate buffer solution (pH: 5.5). The starch suspension was modified using a combination of AM and GAM and incubated in a water-bath thermostatic oscillator at 50 °C for 15 min for preheating. Further, 5 mL of 4 % NaOH solution was added to quench the reaction and obtain a precipitate. The mixture was then centrifuged at 3500×*g* for 10 min and washed with distilled water.

Subsequently, the sediment was dried using different methods—FD, SCD, SPD, and HD. The prepared porous maize and kudzu starch samples obtained via enzymatic hydrolysis were labeled as FDM, SCDM, SPDM, and HDM (samples obtained from maize) and FDK, SCDK, SPDK, and HDK (samples obtained from kudzu).

2.3. Drying methods

The porous maize and kudzu starch samples were prepared using HD, FD, SPD, and SCD, as described below.

2.3.1. HD

The porous starch samples were subjected to HD (BPG-9050AH, Shanghai Yiheng, China) under appropriate parameters, with the reaction time and drying temperature being 8 h and 60°C-80 °C, respectively, and the samples were crushed using an 80-mesh sieve for further use. The resultant porous starch samples were designated as HDK and HDM and stored in a desiccator containing dried allochronic silica gel at a temperature of 25 °C [18]. After HD, the moisture content of the samples was 6.30 % ± 0.16 %, as determined

using a Karl Fischer moisture meter.

2.3.2. SPD

To obtain SPD-treated samples, the porous starch samples were treated using a bench-top spray dryer (SD1500, Shanghai Triowin Tech Co., Ltd., Shandong, China). Slurry containing the porous samples was fed into an atomizer for dispersion into fine droplets, followed by rapid solvent evaporation through heat exchange with hot air to yield dry porous starch. The feed flow rate and inlet temperature were set to 15.4 mL/min and 100 °C ± 5 °C, respectively. The powders were collected using a cyclone collector, loaded into a product collector, and labeled as SPDK and SPDM. The last step in SPD was the collection of the particles and their storage in a desiccator containing dried allochronic silica gel at 25 °C [19]. After SPD, the moisture content of the porous starch samples was 6.50 % ± 0.15 %, as determined using the Karl Fischer moisture meter.

2.3.3. FD

The porous maize and kudzu starch samples (5 g) were dried in a freeze dryer (LGJ-10, Song yuan, China). The samples were prefrozen under the following three conditions: at a temperature of −20 °C, at a temperature of −80 °C, and in liquid nitrogen. However, no notable differences in the properties of the starch samples were observed after subsequent drying (data not shown). The drying cycle lasted for 24 h, and the samples stored in the desiccator were labeled as FDM and FDK [20]. After FD, the moisture content of the porous starch samples was 7.51 % ± 0.13 %, as determined using the Karl Fischer moisture meter.

2.3.4. SCD

In SCD (HISMART-250CPD, Suzhou, China), carbon dioxide was used as the supercritical fluid, which extracted liquid from the hydrogel rather than letting it evaporate. The materials to be dried were obtained by replacing the water in the samples with ethanol using the solvent exchange procedure; subsequent drying involved the use of the supercritical-carbon-dioxide technology [21]. The samples were placed in the pressure chamber of the drying instrument, and the desired mode was selected and relevant parameters were adjusted. After cooling, liquid carbon dioxide was introduced into the chamber until its critical pressure was reached. Subsequently, the samples were heated above the critical temperature and carbon dioxide was discharged through a pipeline. Finally, the products were stored in a desiccator containing dried allochronic silica gel at 25 °C and labeled as SCDK and SCDM. After SCD, the moisture content of the porous starch samples was 6.17 % ± 0.13 %, as determined using the Karl Fischer moisture meter.

2.4. Morphological analysis of starch granules

Scanning electron microscopy (SEM; FEI NANO450) was employed to observe the microstructure of the porous maize and kudzu starch samples subjected to the drying methods. The samples were stuck on a stage using double-sided tape and coated with gold in a vacuum evaporator. Subsequently, micrographs were captured at 4000 × magnification [22].

2.5. Iodine blue spectrophotometry

The porous starch samples were accurately weighed (0.25 g) and 50 mL of distilled water was added, followed by continuous stirring at 65 °C for 5 min. The resulting solution was filtered, and 5 mL of the filtrate was transferred to a 50-mL volumetric flask, followed by the addition of 1 mL of a 0.02 mol/L standard iodine solution to fix the volume. Notably, 1 mL of the 0.02 mol/L standard iodine solution was first added into a tube and then into the 50 mL flask as a blank for zero adjustment; subsequently, the absorbance value of the samples was measured at 650 nm [23,24].

$$\text{Iodine Blue Value} = A_{650nm} \times 54.2 + 5$$

2.6. Crystalline features

The crystalline structure of the porous maize and kudzu starch samples was determined via X-ray diffraction (XRD; Smart Lab-SE). Diffraction patterns were obtained in the 2θ range of 5°–90° [25].

2.7. Fourier-transform infrared spectroscopy

The porous maize and kudzu starch samples (4 mg) and potassium bromide (400 mg) were evenly mixed and analyzed via Fourier-transform infrared spectroscopy (FTIR; Bruker Optik GmbH, Ettlingen, Germany). The samples were analyzed in the wavenumber range of 4000–500 cm^{-1} [26].

2.8. Granular size distribution

Particle size of the porous starch samples was measured by the BT-9300ST laser particle size analyzer (Dandong Better Instrument Co., LTD, China). Starch solutions (2 %) were prepared by pipetting the porous maize and kudzu starch samples in deionized water,

followed by sonicating for 5 min. Subsequently, the shade rate of the porous starch solutions was set to 8%–12 % [27]. Furthermore, the employed instrument automatically averaged the results of three measurements.

2.9. Thermal property measurements

The porous maize and kudzu starch samples were heated at 0°C-200 °C (10 °C/min) for analysis via differential scanning calorimetry (DSC; Q2000, TA Instruments, USA).

2.10. Absorption capacity

2.10.1. Water absorbency

The porous starch samples (1 g) were accurately weighed into 15 mL centrifuge tubes (M_1), to which 10 mL of distilled water was added; they were vortexed for 1 min and then allowed to stand for 30 min [28]. Subsequently, the samples were centrifuged at 35,000 r/min for 10 min, the supernatant was pipetted out, and the total weights of the precipitates and tubes were weighed (M_2). Measurements were conducted thrice in parallel for each sample set. The absorption rate of water was calculated using the following equation:

$$\textit{Water Absorption}\ (\%) = M_2 - M_1 - M_0/M_0 \times 100\%,$$

where M_2 and M_0 are the weights of the starch sample before and after absorption (g), respectively, M_1 is the weight of the dry centrifuge tube (g), and W is the water absorption of the sample (%).

2.10.2. Dye absorbency

Dye-absorption experiments were conducted based on the method proposed by Guo et al. [29], with some modifications. Dried starch sample particles (0.1 g) were added to a 10 mL solution of methylene blue (MB) or neutral red (NR) and gently stirred for 2 h to absorb the dye. Subsequently, the mixtures were centrifuged at 3,000 rpm for 5 min, and the absorbance of the supernatant was measured using a UV-754 PC spectrophotometer (Shanghai Jinghua, P.R. China) at 665 and 552 nm.

The dye-absorption capacity was calculated using the following equation:

$$\textit{Dye Absorption}\ (\mathrm{mg/g}) = (C_1 - C_2) \times V/m,$$

where C_1 and C_2 are the concentrations of MB before and after absorption (mg/L), respectively; V is the volume of MB (L); and m is the

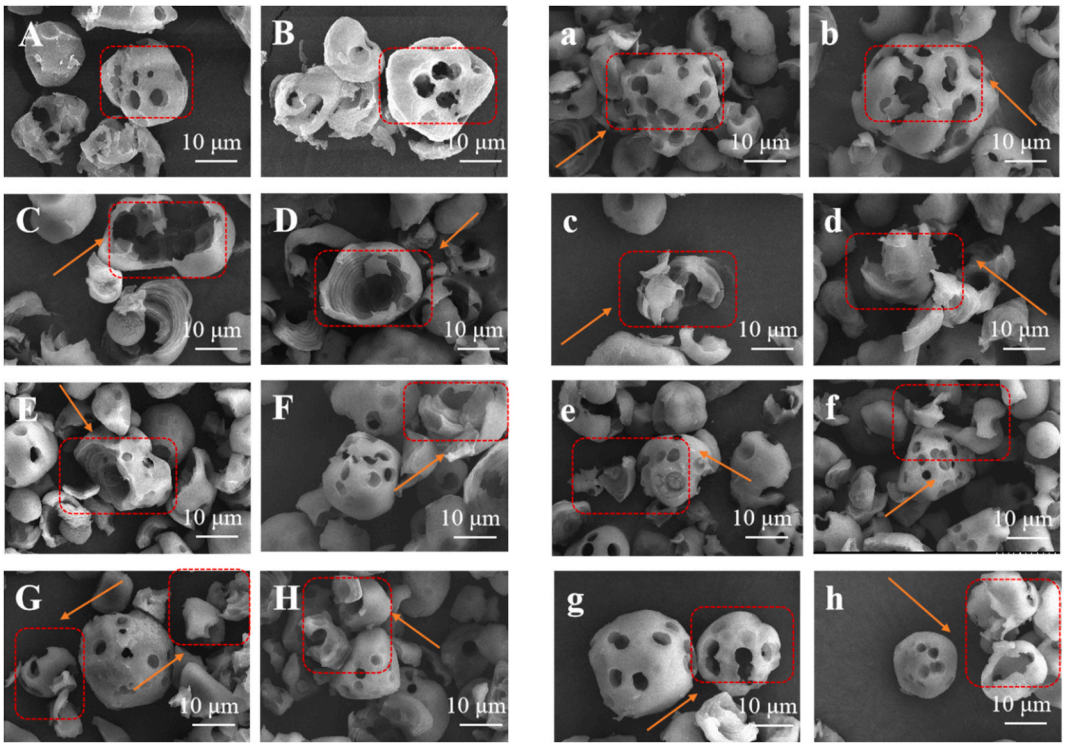

Fig. 1. SEM micrographs of porous maize and kudzu starch samples produced using various drying methods (magnification: 4000 ×). (A–B) SCDK, (C–D) HDK, (E–F) FDK, (G–H) SPDK, (a–b) SCDM, (c–d) HDM, (e–f) FDM, and (g–h) SPDM.

sample weight (g).

2.11. Porosity characteristics

In this experiment, the porous kudzu and maize starch samples (30 mg) were determined by low-temperature liquid nitrogen adsorption at −195.8 °C using the Brunauer-Emmett-Teller (BET, Autosor-iQ, Quantanchrome INSTRUMENTS, USA) [30]. The relative pressure ranged from 0.01 to 1.0 MPa. The degassing temperature of the sample was 100–200 °C, the time was 6–10 h, the adsorbent was porous starch and the adsorbent mass was nitrogen. The specific surface area and pore diameter were calculated by the BET equation for the determination of the adsorbent.

2.12. Determination of total starch content and amylose ratio

The content of total starch was determined using AOAC methods [31], and the amylose ratio in starch was analyzed by the iodine binding method [32], with only a few modifications.

2.13. Statistical analysis

The obtained results are reported as mean and standard deviation of at least triplicate measurements, except for XRD measurements, which were performed only once. All data were analyzed through one-way analysis of variance using the SPSS software.

3. Results and discussion

3.1. Granular morphology

Fig. 1 presents the SEM micrographs of the granules of the porous starch samples at a magnification of 4000 × . Clearly, the number and size of the pores in the granules of the samples dried using various drying methods were different.

As shown in Fig. 1, the surface of the maize and kudzu starch samples was formed as a porous structure due to the action of enzymes. Clearly, HD generated some holes and fissures; meanwhile, these granular structures collapsed in an irregular manner upon treatment (Fig. 1C, D and c, d). The cracks and debris in the HD-treated starch might have been because starch molecules were completely in contact with water molecules during HD; as the drying temperature increased, the internal dissociation of starch molecules produced a powerful force to break the surface of the granules, resulting in forced deformation of the granules [33]. Similarly, the micrographs of the porous starch obtained via FD (Fig. 1E, F and e, f) and SPD (Fig. 1G, H and g, h) also showed some irregular collapses and disintegrations, but there are fewer collapses compared with HD-treated samples.

The SEM micrographs of the SCD-treated samples (Fig. 1A, B and a, b) showed that the number of pores produced via FD and SCD was similar. However, the pores produced using SCD were larger and had a larger specific surface area than those produced using other methods. This fact could be directly related to the absence of surface tension during the drying process, microstructural changes caused by capillary surface tension in the starch samples, such as pore collapse, are avoided. Therefore, this drying technique can preserve the original microstructure of the material, resulting in structurally intact and uniformly distributed sample particles. The above phenomena imply that SCD is suitable for producing porous starch.

3.2. Iodine blue values of porous starch subjected to different drying methods

The content of free starch can be evaluated based on the iodine blue value [34]. Smaller iodine blue values indicate lower degree of starch breakage and free starch content. As shown in Fig. 2A and B, the iodine blue value of the maize and kudzu porous starch samples after HD was the highest (23.86,19.53, respectively); with increasing temperature, the starch granules were severely broken and the

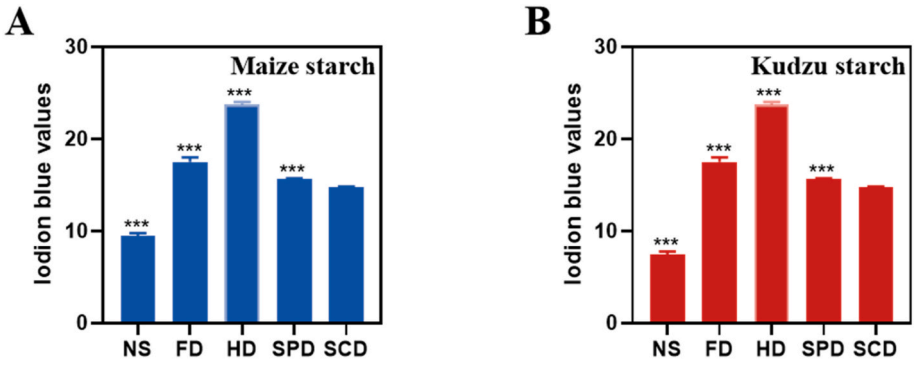

Fig. 2. Effect of the four drying methods on the iodine blue value of the porous maize (A) and kudzu starch (B) samples.

free starch precipitated. The SCD-treated maize and kudzu porous starch had the lowest iodine blue value (12.51,12.73, respectively), indicating that SCD aided in the preservation of the integrity of starch granules and produced uniform, complete porous starch. As seen, there are significant differences between the samples dried using SCD and those dried by the other three drying methods. This was consistent with the result obtained through SEM analysis.

3.3. X-Ray diffraction

XRD patterns and relative crystallinity (RC%) values of the porous maize and kudzu starch samples obtained via different drying methods are presented in Fig. 3. The kudzu starch sample exhibited a C-type crystal pattern, characterized by strong intensity peaks at 2θ values of 15.7° and 17.4° along with a few minor reflections at approximately 5.6° and 15.3° (Fig. 3A), consistent with the results of previous studies [35,36]. Several main peaks were observed at 2θ values of 15.3°, 17.8°, 18.2°, and 23.5° in the diffractogram for the maize starch sample (Fig. 3B), indicating that the sample exhibited an A-type crystal structure. Similar results were reported for other types of maize starches [37]. The diffractograms of the samples subjected to the four drying methods did not exhibit any substantial variations (Fig. 3). This indicates that the different drying methods only changed the intensity of the peaks, while the crystal type remained the same.

As shown in Fig. 3, compared with the other samples, the SCD-treated sample showed the highest peak intensity for crystalline domains. Denser particles with a high crystalline fraction density in the SCD-treated porous starch particles might have been the reason for such high diffraction peak intensity. In addition to a reduction in the intensity of the characteristic diffraction peaks of porous maize and kudzu starch in the HD-treated samples, their crystallinity also considerably decreased. Kan et al. [38] suggested that the partial gelatinization and double-helical movement of starch during drying may disrupt starch crystallites and destroy crystalline regions within starch granules.

3.4. Thermal analysis

As shown in Fig. 4, the thermal properties of the porous maize and kudzu starch samples prepared using different drying methods were determined via DSC.

Fig. 4C and C1 depicts SCD-treated samples exhibited higher gelatinization temperatures (T_o, T_p, and T_c) and gelatinization

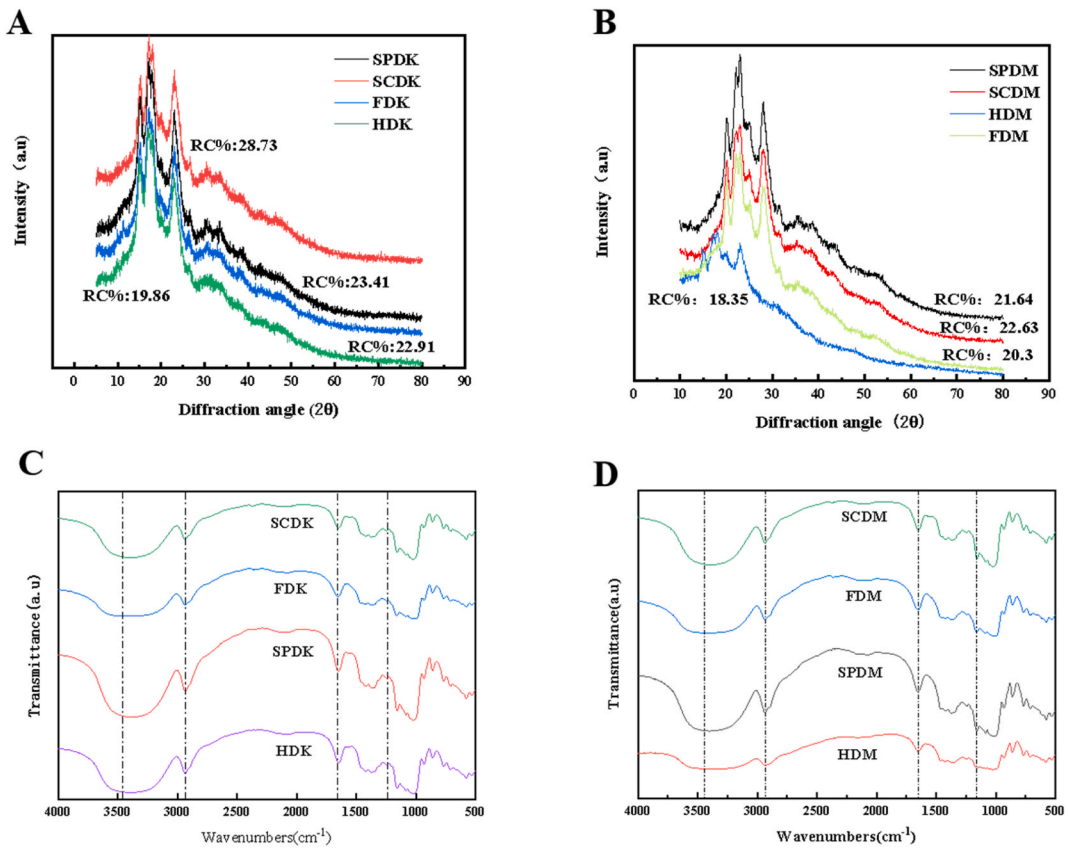

Fig. 3. X-Ray diffractograms (A, B) and Fourier-transform infrared spectra (C, D) of the porous kudzu and maize starch samples.

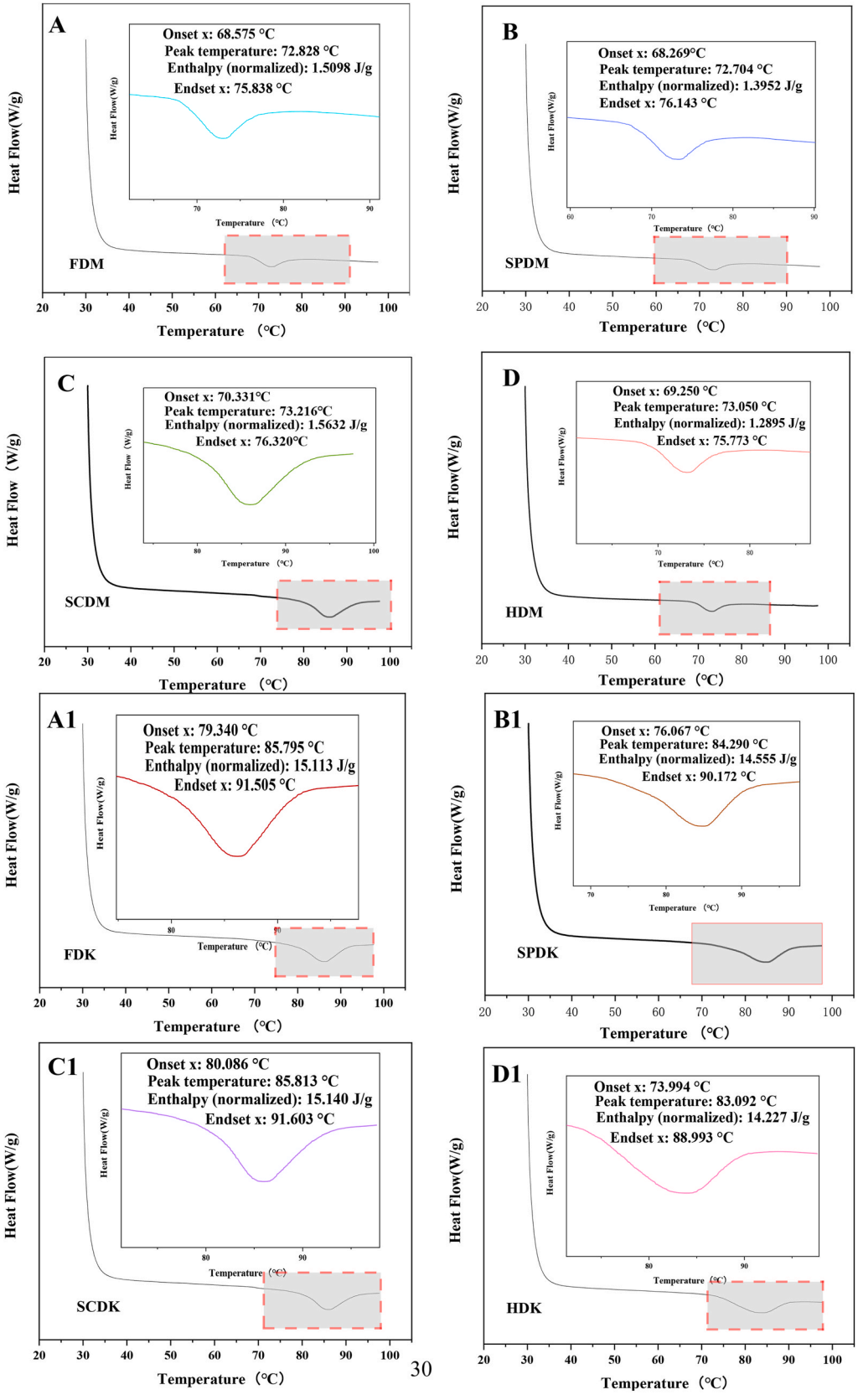

(caption on next page)

Fig. 4. Differential scanning calorimetry thermograms of the porous kudzu and maize starch samples treated with the four drying methods: (A) FDM, (B) SPDM, (C) SCDM, (D) HDM, (A1) FDK, (B1) SPDK, (C1) SCDK, (D1) HDK.

enthalpy (ΔH) than the HD-, SPD-, and FD-treated samples. HD considerably decreased the gelatinization temperature and ΔH values of the porous maize and kudzu starch samples (Fig. 4D and D1), indicating a disruption in the crystalline structure or double-helical movement of the starch granules during HD, which is consistent with the XRD and FTIR results. Zhang et al. [13] reported that higher temperatures employed in the drying process lead to lower pasting temperatures and enthalpies of the starch samples.

3.5. FTIR spectroscopic analysis

FTIR spectra of the samples after undergoing different drying treatments are presented in Fig. 3C and D. All samples exhibited similar characteristic peaks at 3463.6, 2946.3, 1659.3, 1377.6, 1148.6, 1064.3, and 924.5 cm^{-1}.

According to previous research, the absorbance ratio of 1047 cm^{-1}/1022 cm^{-1} can be used to evaluate the degree of short-term ordering in starch granules [39,40].

As shown in Table 1, the peak ratios of 1047 cm^{-1}/1022 cm^{-1} for the starch samples treated using HD, FD, SPD, and SCD were 1.17, 1.22, 1.44, and 1.54 (for maize) and 1.53, 1.61, 1.64, and 1.82 (for kudzu), respectively.

SCD-treated samples showed the highest peak ratio of the 1047 cm^{-1}/1022 cm^{-1}, indicating that the SCD samples had the highest ordering degree. Nonetheless, HD reduced the ordered structure of the starch, consistent with the XRD results. This phenomenon may have occurred owing to the melting of amylose chains and deformation of partial crystalline regions at high temperatures [41].

3.6. Particle size distribution

Particle size is an important parameter that affects the physical properties of powders, such as stability, handling feasibility, and storage capacity. As indicated in Table 1, compared with those of the native maize and kudzu starches, reduction in the D (3,2) and D (4,3) values of the treated porous starch samples was observed.

As shown in Table 1, the volume-weighted mean diameter (D (4,3)) of the porous maize and kudzu starch samples dried using different methods ranged from 8.845 (SCD) to 11.61 μm (HD) and from 8.012 (SCD) to 11.76 μm (HD), respectively. The d (0.1), d (0.5), and d (0.9) values of the SCD-treated porous starch samples were the lowest among all samples, while the sample prepared using HD exhibited coarseness and higher density than those of the other samples (Table 1). The variation in particle size distribution of porous starch granules after four drying methods in the present study could be due to water content differences. A previous study has showed that high moisture content in porous starch can cause aggregation of granules into lumps, thereby affecting particle size [42], which was consistent with the results obtained through SEM analysis.

3.7. Absorption capacity

Absorption capacity is an essential performance index of porous starches because the pores in starches are often used as carriers to

Table 1
Particle size parameters, the peak ratio of 1047 cm^{-1}/1022 cm^{-1} and adsorption capacity of the porous starches studied herein.

Sample	Treatment	Water (%)	MB (mg/g)	NR (mg/g)	D (0.1) (v/v, μm)	D (0.5) (v/v, μm)	D (0.9) (v/v, μm)	Surface-weighted mean (μm, D (3,2))	Volume-weighted mean (μm, (4,3))	1047 cm^{-1}/1022 cm^{-1}
Kudzu	NS	109.62 ± 0.47	30.71 ± 0.08	35.59 ± 0.27	9.119 ± 0.18	15.15 ± 0.06	21.73 ± 0.03	10.85 ± 0.07	15.15 ± 0.05	–
	FD	122.59 ± 0.32*	81.23 ± 0.41**	83.57 ± 0.23***	2.713 ± 0.13	9.142 ± 0.12	2.913 ± 0.07	5.539 ± 0.04	9.641 ± 0.06	1.44 ± 0.02
	SPD	119.43 ± 0.12**	42.05 ± 0.95***	50.30 ± 0.11***	2.713 ± 0.13	9.142 ± 0.08	15.34 ± 0.13	5.539 ± 0.05	9.206 ± 0.04	1.22 ± 0.64
	HD	125.37 ± 0.58***	68.05 ± 0.55**	73.07 ± 0.08**	3.201 ± 0.26	10.36 ± 0.12	18.50 ± 0.17	5.891 ± 0.09	11.61 ± 0.06	1.17 ± 0.75
	SCD	120.90 ± 0.73	90.63 ± 0.41	90.98 ± 1.02	2.386 ± 0.19	8.387 ± 0.18	15.69 ± 0.14	5.063 ± 0.11	8.845 ± 0.16	1.54 ± 0.07
Maize	NS	113.49 ± 0.12	52.15 ± 0.01	53.37 ± 0.16	2.278 ± 0.19	7.728 ± 0.12	21.62 ± 0.04	4.770 ± 0.11	12.72 ± 0.05	–
	FD	126.59 ± 0.54*	87.83 ± 0.01**	90.48 ± 0.02**	2.546 ± 0.17	7.895 ± 0.16	13.96 ± 0.17	5.054 ± 0.06	9.372 ± 0.13	1.57 ± 0.16
	SPD	122.43 ± 0.47***	59.37 ± 0.47***	65.18 ± 0.16***	2.495 ± 0.13	7.898 ± 0.07	13.91 ± 0.14	5.029 ± 0.19	9.158 ± 0.14	1.53 ± 0.18
	HD	131.04 ± 0.47***	75.53 ± 0.47***	79.34 ± 0.33***	2.246 ± 0.07	7.884 ± 0.11	20.17 ± 0.08	4.814 ± 0.10	11.76 ± 0.08	1.64 ± 0.11
	SCD	125.43 ± 0.14	100.26 ± 0.47	103.42 ± 0.25	1.572 ± 0.13	7.682 ± 0.09	14.15 ± 0.06	4.314 ± 0.06	8.012 ± 0.02	1.82 ± 0.13

All values were expressed as the mean ± SD; n = 3; *P < 0.05, **P < 0.01, ***P < 0.001significantly different from SCD).

transport drugs and encapsulate bioactive materials [43]. Herein, three liquids—water, MB, and NR—were used to study the absorption capacity of the porous maize and kudzu starch samples; the results are presented in Fig. 5.

The water-absorption capacity of the porous starch samples is shown in Fig. 5A and B and Table 1. The variation in the water-absorption capacity may be related to the variation in the contents of hydrophilic components and the properties of the samples. HD-treated samples showed the highest water-absorption capacity of 125.31 % and 131.04 % (for the porous kudzu and maize starch

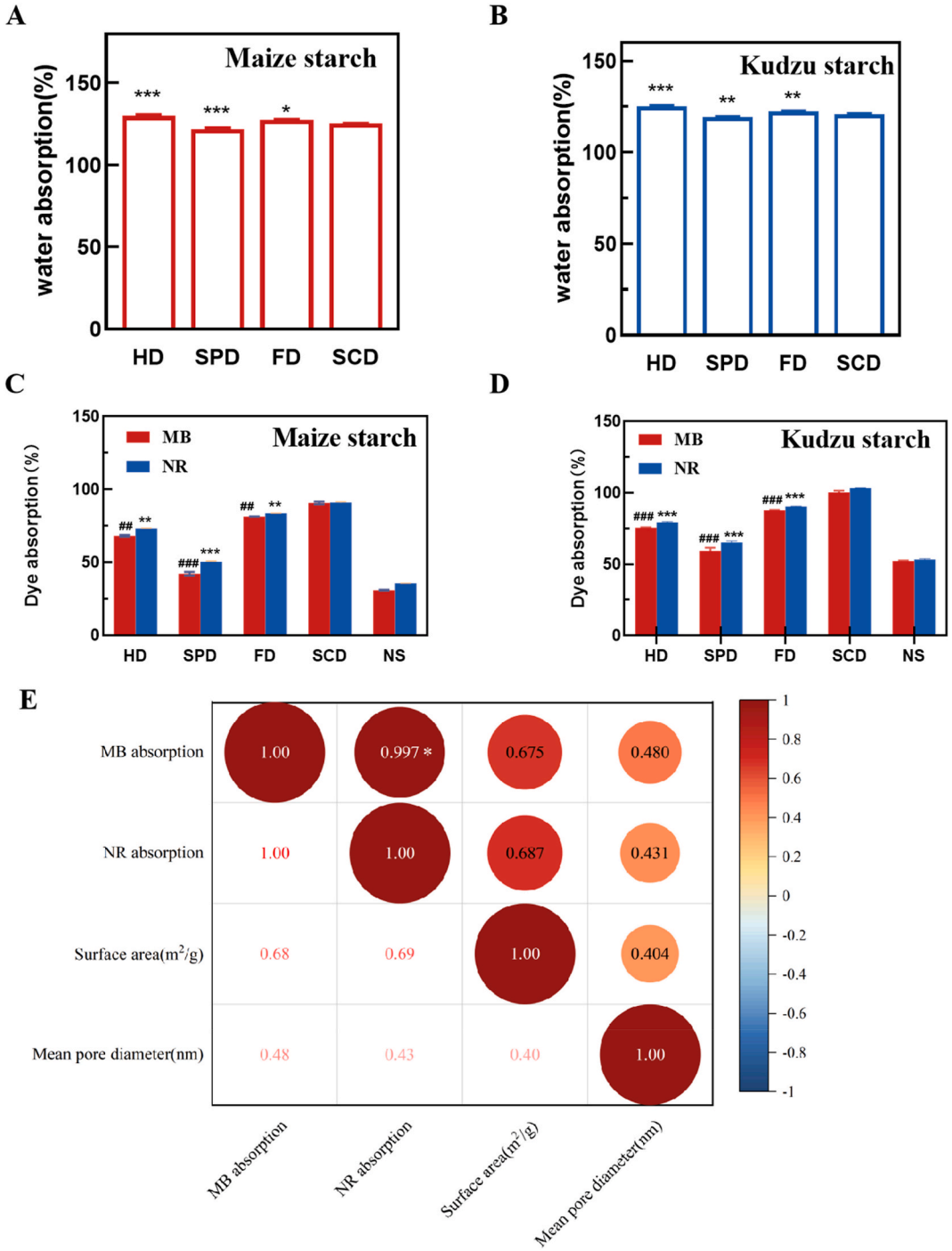

Fig. 5. Water- and dye-absorption capacities of porous maize (A, C) and kudzu (B, D) starches prepared using the four drying methods: HD, SPD, FD, and SCD. Heatmap of the distribution of correlation coefficients between the dye absorption, surface and pore size of the kudzu and maize porous starch (E).

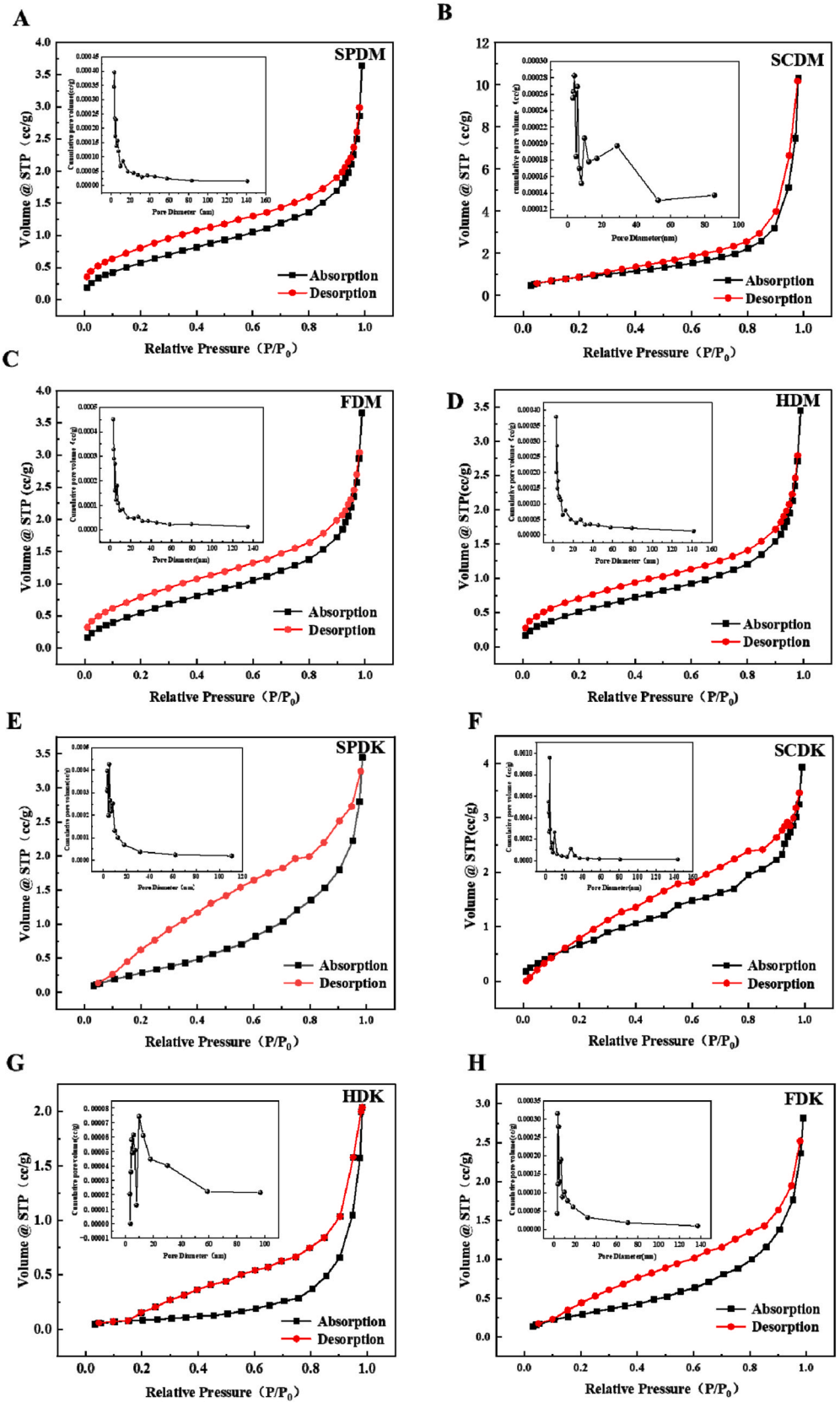

(caption on next page)

Fig. 6. Differential curves of the pore volume distribution and cumulative-pore-volume curves as well as adsorption–desorption curves of porous maize and kudzu starch samples synthesized using different drying methods. (A) SPDM, (B) SCDM, (C) FDM, (D) HDM, (E) SPDK, (F) SCDK, (G) FDK, and (H) HDK.

samples, respectively), followed by the FD-treated samples. This may be attributed to the fact that starch can gelatinize during HD, which enhances its water-absorption capacity. Higher degree of gelatinization leads to higher water-absorption capacity of porous starch [44].

The dye-absorption capacity of the porous starch samples was also related to their properties. Fig. 5C and D and Table 1 present the dye-absorption capacities of the porous starch samples. The dye-absorption capacities of the kudzu and maize starch samples produced using SCD were 90.63 % (MB) and 125.43 % (MB), respectively, and 90.98 % (NR) and 100.26 % (NR), respectively.

During SCD, three continuous flow events of supercritical CO_2 helped remove the solvent, which made its way through the starch granules, forming small pores and increasing the surface contact area of the porous starch, with minimal damage to the granules. This explains why the dye-absorption capacity of the SCD-treated samples was higher than that of the other samples. Moreover, in case the HD, the higher degree of pore collapse decreased the dye-absorption capacity of the sample.

These results, combined with the SEM results, indicate that different drying treatments of the porous starch samples can lead to the formation of a high number of pores and high absorption rate during hydrolysis.

3.8. Specific surface area, pore size, and isothermal adsorption curve

Fig. 6 and Table 2 show the pore diameter and volume distributions of the porous starch samples; the samples exhibited a type-IV isotherm, indicating a mesoporous structure [45].

The surface tension of the liquid or gas during the drying process is a notable factor influencing the formation of continuous and uniform pores in the porous starch, with complete retention of the integrity of the starch granules after an appropriate drying process. Table 2 indicates that the SCD-treated samples showed considerably higher surface areas (2.943 and 3.139 m^2/g corresponding to kudzu and maize, respectively) than those prepared using other methods. This may be attributed to the negligible surface tension experienced by the samples during SCD. This phenomenon demonstrated that a process with the lowest surface tension is beneficial for producing porous starch with a high porosity. Based on the results of the current study, Specific surface area of porous starch and dye absorption exhibited a positive relationship, which may be attributed to the porous structure and surface characteristics of the particle size, where larger surface area with more pore structures contributed to a high dye absorption.

3.9. Total starch content and amylose ratio of starch

The total starch content and amylose ratio of maize and kudzu porous starches after HD, FD, SCD, SPD treatment is presented in Table 3. The ratio of SCD, FD, SPD-treated starch amylose was 22.02 %, 20.68 % and 19.51 %; 16.85 %, 15.02 % and 15.02 % corresponding to kudzu and maize, respectively. The amylose content of the SCD was significantly different ($p > 0.05$) compared with that of the FD and SPD sample. Additionally, the maize and kudzu starch content of the HD sample decreased to 15.33 % and 12.41 %. The results indicate that high-temperature drying disrupts the amylose structure in the center and non-crystalline regions of starch granules, damaging the lamellar structure and leading to the extraction or dissolution of amylose, resulting in a decrease in amylose content.

4. Conclusions

After undergoing different drying methods, maize and kudzu porous starches exhibit significant differences in terms of apparent composition, functionality, and morphology. After HD, a large number of cracks and debris were observed in the starch granules. The degree of fragmentation of starch particles after FD and SPD is less than that of HD. Nevertheless, SCD-treated samples exhibited the highest degree of porosity, surface area, dye absorption capacity and integrity of particles.

Our experimental results showed that SCD is a productive method for preparing porous starch with small pores and minimal

Table 2
Parameters obtained from nitrogen sorption experiments at 77 K of porous maize and kudzu starch samples treated using the four drying methods.

Sample	Treatment	Specific surface area (m^2/g)	Mean pore diameter (nm)	R^2 (BET)
Kudzu	FD	1.313 ± 0.06**	4.308 ± 0.07*	0.999112 ± 0.02
	SPD	1.164 ± 0.13**	3.409 ± 0.08**	0.997287 ± 0.01
	HD	0.909 ± 0.05***	3.065 ± 0.07**	0.999681 ± 0.01
	SCD	2.943 ± 0.10	4.586 ± 0.13	0.999752 ± 0.04
	FD	2.322 ± 0.07**	3.452 ± 0.06**	0.999223 ± 0.01
Maize	SPD	1.986 ± 0.12***	3.410 ± 0.1**	0.999625 ± 0.07
	HD	1.709 ± 0.15***	3.067 ± 0.14***	0.999545 ± 0.05
	SCD	3.193 ± 0.09	4.769 ± 0.07	0.999897 ± 0.04

All values were expressed as the mean ± SD; n = 3; *P < 0.05, **P < 0.01, ***P < 0.001significantly different from SCD).

Table 3
The total starch content and amylose of starch ratio.

Sample	Treatment	Starch purity (%)	Amylose content (%)
Kudzu	NS	85.9 ± 0.02	28.12 ± 0.07
	FD	85.9 ± 0.02	20.68 ± 0.02**
	SPD	85.9 ± 0.02	19.51 ± 0.04***
	HD	85.9 ± 0.02	15.33 ± 0.06***
	SCD	85.9 ± 0.02	22.02 ± 0.01
Maize	NS	87.63 ± 0.05	26.59 ± 0.05
	FD	87.63 ± 0.05	15.02 ± 0.03**
	SPD	87.63 ± 0.05	13.86 ± 0.03***
	HD	87.63 ± 0.05	12.41 ± 0.05***
	SCD	87.63 ± 0.05	16.85 ± 0.03

All values were expressed as the mean ± SD; n = 3; *P < 0.05, **P < 0.01, ***P < 0.001 significantly different from SCD).

damage to the microstructure. Thus, relatively stable porous starch can be produced through enzymatic hydrolysis followed by SCD. This study provides useful information regarding the effect of different drying methods on the functional and physicochemical properties of porous starch and valuable guidance reference for selecting the appropriate drying method for its application in different fields.

Funding

This research did not receive any specific grant from funding agencies in the public, commercial, or not-for-profit sectors.

Data statement

All data used/generated in the study are presented in the main text.

CRediT authorship contribution statement

Yuanyuan Zhao: Writing – original draft, Methodology, Formal analysis, Data curation, Conceptualization. **Simo Qiao:** Methodology, Investigation, Conceptualization. **Xiaohui Zhu:** Formal analysis, Data curation. **Jinnan Guo:** Formal analysis, Data curation. **Guanqun Peng:** Formal analysis, Data curation. **Xiaoxia Zhu:** Investigation, Formal analysis. **Ruolan Gu:** Methodology, Formal analysis. **Zhiyun Meng:** Formal analysis, Data curation. **Zhuona Wu:** Methodology, Formal analysis. **Hui Gan:** Methodology, Conceptualization. **Dou Guifang:** Writing – review & editing, Data curation, Conceptualization. **Yiguang Jin:** Writing – review & editing, Resources. **Shuchen Liu:** Supervision, Investigation. **Yunbo Sun:** Writing – review & editing, Methodology, Conceptualization.

Declaration of competing interest

The authors declare that they have no known competing financial interests or personal relationships that could have appeared to influence the work reported in this paper.

References

[1] J. Chen, Y. Wang, J. Liu, X. Xu, Preparation, characterization, physicochemical property and potential application of porous starch: a review, Int. J. Biol. Macromol. 148 (2020) 1169–1181, https://doi.org/10.1016/j.ijbiomac.2020.02.055.
[2] C. Belingheri, A. Ferrillo, E. Vittadini, Porous starch for flavor delivery in a tomato-based food application, LWT - Food Sci. Technol. (Lebensmittel-Wissenschaft -Technol.) 60 (2015) 593–597, https://doi.org/10.1016/j.lwt.2014.09.047.
[3] H. Wang, J. Lv, S. Jiang, B. Niu, M. Pang, S. Jiang, Preparation and characterization of porous corn starch and its adsorption toward grape seed proanthocyanidins, Starch Stärke 68 (2016) 1254–1263, https://doi.org/10.1002/star.201600009.
[4] S.A. Razzak, M.O. Faruque, Z. Alsheikh, L. Alsheikhmohamad, D. Alkuroud, A. Alfayez, S.M.Z. Hossain, M.M. Hossain, A comprehensive review on conventional and biological-driven heavy metals removal from industrial wastewater, Environmental Advances 7 (2022) 100168, https://doi.org/10.1016/j.envadv.2022.100168.
[5] D.N. Hj Latip, H. Samsudin, U. Utra, A.K. Alias, Modification methods toward the production of porous starch: a review, Crit. Rev. Food Sci. Nutr. 61 (2021) 2841–2862, https://doi.org/10.1080/10408398.2020.1789064.
[6] A. Dura, W. Błaszczak, C.M. Rosell, Functionality of porous starch obtained by amylase or amyloglucosidase treatments, Carbohydr. Polym. 101 (2014) 837–845, https://doi.org/10.1016/j.carbpol.2013.10.013.
[7] R. He, W.T. Shang, Y.G. Pan, D. Xiang, Y.H. Yun, W.M. Zhang, Effect of drying treatment on the structural characterizations and physicochemical properties of starch from canistel (Lucuma nervosa A.DC), Int. J. Biol. Macromol. 167 (2021) 539–546, https://doi.org/10.1016/j.ijbiomac.2020.12.008.
[8] P. Correia, M.L. Beirão-da-Costa, Effect of drying temperatures on starch-related functional and thermal properties of chestnut flours, Food Bioprod. Process. 90 (2012) 284–294, https://doi.org/10.1016/j.fbp.2011.06.008.
[9] X. Xu, L. Zhang, Y. Feng, C. Zhou, A.E.A. Yagoub, H. Wahia, H. Ma, J. Zhang, Y. Sun, Ultrasound freeze-thawing style pretreatment to improve the efficiency of the vacuum freeze-drying of okra (Abelmoschus esculentus (L.) Moench) and the quality characteristics of the dried product, Ultrason. Sonochem. 70 (2021) 105300, https://doi.org/10.1016/j.ultsonch.2020.105300.

[10] A. Nascimento, M.E.R.M. Cavalcanti-Mata, M.E. Martins Duarte, M. Pasquali, H.M. Lisboa, Construction of a design space for goat milk powder production using moisture sorption isotherms, J. Food Process. Eng. 42 (2019) e13228, https://doi.org/10.1111/jfpe.13228.
[11] S. Basak, R.S. Singhal, The potential of supercritical drying as a "green" method for the production of food-grade bioaerogels: a comprehensive critical review, Food Hydrocolloids 141 (2023) 108738, https://doi.org/10.1016/j.foodhyd.2023.108738.
[12] S. Apinan, I. Yujiro, Y. Hidefumi, F. Takeshi, P. Myllärinen, P. Forssell, K. Poutanen, Visual observation of hydrolyzed potato starch granules by α-amylase with confocal laser scanning microscopy, Starch - Stärke 59 (2007) 543–548, https://doi.org/10.1002/star.200700630.
[13] B. Zhang, K. Wang, J. Hasjim, E. Li, B.M. Flanagan, M.J. Gidley, S. Dhital, Freeze-drying changes the structure and digestibility of B-polymorphic starches, J. Agric. Food Chem. 62 (2014) 1482–1491, https://doi.org/10.1021/jf405196m.
[14] S. Ferreira, T. Araujo, N. Souza, L. Rodrigues, H.M. Lisboa, M. Pasquali, G. Trindade, A.P. Rocha, Physicochemical, morphological and antioxidant properties of spray-dried mango kernel starch, Journal of Agriculture and Food Research 1 (2019) 100012, https://doi.org/10.1016/j.jafr.2019.100012.
[15] X. Han, H. Wen, Y. Luo, J. Yang, W. Xiao, X. Ji, J. Xie, Effects of α-amylase and glucoamylase on the characterization and function of maize porous starches, Food Hydrocolloids 116 (2021) 106661, https://doi.org/10.1016/j.foodhyd.2021.106661.
[16] F. Zou, T. Budtova, Tailoring the morphology and properties of starch aerogels and cryogels via starch source and process parameter, Carbohydr. Polym. 255 (2021) 117344, https://doi.org/10.1016/j.carbpol.2020.117344.
[17] Z. Davoudi, M.H. Azizi, M. Barzegar, Porous corn starch obtained from combined cold plasma and enzymatic hydrolysis: microstructure and physicochemical properties, Int. J. Biol. Macromol. 223 (2022) 790–797, https://doi.org/10.1016/j.ijbiomac.2022.11.058.
[18] S. Barua, M. Rakshit, P.P. Srivastav, Optimization and digestogram modeling of hydrothermally modified elephant foot yam (Amorphophallus paeoniifolius) starch using hot air oven, autoclave, and microwave treatments, LWT 145 (2021) 111283, https://doi.org/10.1016/j.lwt.2021.111283.
[19] B. Guo, C. Zhu, Z. Huang, R. Yang, C. Liu, Microcapsules with slow-release characteristics prepared by soluble small molecular starch fractions through the spray drying method, Int. J. Biol. Macromol. 200 (2022) 34–41, https://doi.org/10.1016/j.ijbiomac.2021.12.137.
[20] H. Hashemilar, H. Jafarizadeh-Malmiri, O. Ahmadi, N. Jodeiri, Enzymatically preparation of starch nanoparticles using freeze drying technique – gelatinization, optimization and characterization, Int. J. Biol. Macromol. 237 (2023) 124137, https://doi.org/10.1016/j.ijbiomac.2023.124137.
[21] Y. Wang, Y. Su, W. Wang, Y. Fang, S.B. Riffat, F. Jiang, The advances of polysaccharide-based aerogels: preparation and potential application 16, Carbohydr. Polym. 226 (2019) 115242, https://doi.org/10.1016/j.carbpol.2019.115242.
[22] M. Wang, J. Chen, S. Chen, X. Ye, D. Liu, Inhibition effect of three common proanthocyanidins from grape seeds, peanut skins and pine barks on maize starch retrogradation, Carbohydr. Polym. 252 (2021) 117172, https://doi.org/10.1016/j.carbpol.2020.117172.
[23] W.R. Morrison, B. Laignelet, An improved colorimetric procedure for determining apparent and total amylose in cereal and other starches, J. Cereal. Sci. 1 (1983) 9–20, https://doi.org/10.1016/S0733-5210(83)80004-6.
[24] L. Guo, J. Li, Y. Gui, Y. Zhu, B. Yu, C. Tan, Y. Fang, B. Cui, Porous starches modified with double enzymes: structure and adsorption properties, Int. J. Biol. Macromol. 164 (2020) 1758–1765, https://doi.org/10.1016/j.ijbiomac.2020.07.323.
[25] C. Zhang, S.-Y. Wang, C.-Y. Wu, J.-J. Li, L.-Z. Zhang, Z.-J. Wang, Q.-Q. Liu, J.-Y. Qian, Effect of melting combined with ice recrystallization on porous starch preparation: pore-forming properties, granular morphology, functionality, and multi-scale structures, Food Res. Int. 174 (2023) 113463, https://doi.org/10.1016/j.foodres.2023.113463.
[26] Y. Xie, B. Zhang, M.-N. Li, H.-Q. Chen, Effects of cross-linking with sodium trimetaphosphate on structural and adsorptive properties of porous wheat starches, Food Chem. 289 (2019) 187–194, https://doi.org/10.1016/j.foodchem.2019.03.023.
[27] F.M. Bhat, C.S. Riar, Effect of amylose, particle size & morphology on the functionality of starches of traditional rice cultivars, Int. J. Biol. Macromol. 92 (2016) 637–644, https://doi.org/10.1016/j.ijbiomac.2016.07.078.
[28] Y. Hou, Y. Xia, Y. Pan, S. Tang, X. Sun, Y. Xie, H. Guo, J. Wei, Influences of mesoporous zinc-calcium silicate on water absorption, degradability, antibacterial efficacy, hemostatic performances and cell viability to microporous starch based hemostat, Materials Science and Engineering, C, Materials for Biological Applications 76 (2017) 340–349, https://doi.org/10.1016/j.msec.2017.03.094.
[29] L. Guo, R. Liu, X. Li, Y. Sun, X. Du, The physical and adsorption properties of different modified corn starches, Starch - Stärke 67 (2015) 237–246, https://doi.org/10.1002/star.201400200.
[30] T. Keeratiburana, A.R. Hansen, S. Soontaranon, S. Tongta, A. Blennow, Porous rice starch produced by combined ultrasound-assisted ice recrystallization and enzymatic hydrolysis, Int. J. Biol. Macromol. 145 (2020) 100–107, https://doi.org/10.1016/j.ijbiomac.2019.12.144.
[31]] AOAC Official Methods of Analysis Arlington, VA, 1997.
[32] Z. Yang, X. Xu, R. Singh, L. De Campo, E.P. Gilbert, Z. Wu, Y. Hemar, Effect of amyloglucosidase hydrolysis on the multi-scale supramolecular structure of corn starch, Carbohydr. Polym. 212 (2019) 40–50, https://doi.org/10.1016/j.carbpol.2019.02.028.
[33] D. Liu, W. Tang, Y. Xin, J. Yang, L. Yuan, X. Huang, J. Yin, S. Nie, M. Xie, Comparison on structure and physicochemical properties of starches from adzuki bean and dolichos bean, Food Hydrocolloids 105 (2020) 105784, https://doi.org/10.1016/j.foodhyd.2020.105784.
[34] Y. Hui, H. Shen, X. Yao, et al., Quality analysis of different varieties of potato snowflakes powder, Science and Technology of Food Industry 44 (2023) 356–365, https://doi.org/10.13386/j.issn1002-0306.2022120091.
[35]] Z. Niu, M. Li, X. Hou, D. Qiao, Z. Cheng, L. Zhang, B. Zhang, Shortening growth year improves functional features of kudzu starch by tailoring its multi-scale structure, Int. J. Biol. Macromol. 251 (2023) 126362, https://doi.org/10.1016/j.ijbiomac.2023.126362.
[36] B. Zhang, D. Cui, M. Liu, H. Gong, Y. Huang, F. Han, Corn porous starch: preparation, characterization and adsorption property, Int. J. Biol. Macromol. 50 (2012) 250–256, https://doi.org/10.1016/j.ijbiomac.2011.11.002.
[37] Z. Geng, C. Zongdao, W. Yimin, Physicochemical properties of lotus (Nelumbo nucifera Gaertn.) and kudzu (Pueraria hirsute Matsum.) starches, Int. J. Food Sci. Technol. 42 (2007) 1449–1455, https://doi.org/10.1111/j.1365-2621.2006.01363.x.
[38] L. Kan, Q. Li, S. Xie, J. Hu, Y. Wu, J. Ouyang, Effect of thermal processing on the physicochemical properties of chestnut starch and textural profile of chestnut kernel, Carbohydr. Polym. 151 (2016) 614–623, https://doi.org/10.1016/j.carbpol.2016.06.008.
[39] Y. Luo, Y. Xiao, M. Shen, H. Wen, Y. Ren, J. Yang, X. Han, J. Xie, Effect of Mesona chinensis polysaccharide on the retrogradation properties of maize and waxy maize starches during storage, Food Hydrocolloids 101 (2020) 105538, https://doi.org/10.1016/j.foodhyd.2019.105538.
[40] J. Zhu, W. Sun, Z. Meng, X. Zhu, H. Gan, R. Gu, Z. Wu, G. Dou, Preparation and characterization of a new type of porous starch microspheres (PSM) and effect of physicochemical properties on water uptake rate, Int. J. Biol. Macromol. 116 (2018) 707–714, https://doi.org/10.1016/j.ijbiomac.2018.05.059.
[41] M. González, E.J. Vernon-Carter, J. Alvarez-Ramirez, Y. Carrera-Tarela, Effects of dry heat treatment temperature on the structure of wheat flour and starch in vitro digestibility of bread, Int. J. Biol. Macromol. 166 (2021) 1439–1447, https://doi.org/10.1016/j.ijbiomac.2020.11.023.
[42] H.-M. Liu, Y.-Y. Yan, X.-X. Liu, Y.-X. Ma, X.-D. Wang, Effects of various oil extraction methods on the gelatinization and retrogradation properties of starches isolated from tigernut (Cyperus esculentus) tuber meals, Int. J. Biol. Macromol. 156 (2020) 144–152, https://doi.org/10.1016/j.ijbiomac.2020.03.252.
[43] W. Xiao, H. He, Q. Dong, Q. Huang, F. An, H. Song, Effects of high-speed shear and double-enzymatic hydrolysis on the structural and physicochemical properties of rice porous starch, Int. J. Biol. Macromol. 234 (2023) 123692, https://doi.org/10.1016/j.ijbiomac.2023.123692.
[44] Q. Sun, X. Song, M. Arun S, L. Zhang, X. Yu, C. Zhou, Y. Tang, A.E.A. Yagoub, Effects of blanching drying methods on the structure and physicochemical properties of starch in sweet potato slices, Food Hydrocolloids 127 (2022) 107543, https://doi.org/10.1016/j.foodhyd.2022.107543.
[45] H. Xie, C. Xiang, Y. Li, L. Wang, Y. Zhang, Z. Song, X. Ma, X. Lu, Q. Lei, W. Fang, Fabrication of ovalbumin/κ-carrageenan complex nanoparticles as a novel carrier for curcumin delivery, Food Hydrocolloids 89 (2019) 111–121, https://doi.org/10.1016/j.foodhyd.2018.10.027.